

1 **FENTON-LIKE CATALYST BASED ON A RETICULATED POROUS PEROVSKITE MATERIAL: ACTIVITY**  
2 **AND STABILITY FOR THE ON-SITE REMOVAL OF PHARMACEUTICAL MICROPOLLUTANS IN A**  
3 **HOSPITAL WASTEWATER**

4

5 A. Cruz del Álamo, C. González Gómez, M.I. Pariente, R. Molina, F. Martínez\*

6

7 Department of Chemical and Environmental Technology, ESCET, Rey Juan Carlos University,  
8 28933, Móstoles, Madrid, Spain.

9

10 \*Corresponding author: Fernando Martínez Castillejo

11

12 E-mail address: [fernando.castillejo@urjc.es](mailto:fernando.castillejo@urjc.es)

13

14

15

16

17

18

19

20

21

22

23

24

25

26

27

28 **ABSTRACT**

29 Powder  $\text{LaCu}_{0.5}\text{Mn}_{0.5}\text{O}_3$  perovskite was successfully conformed in a reticulated macroporous  
30 structure to be tested in an up-flow catalytic packed bed reactor as on-site pre-treatment of a  
31 hospital wastewater for the removal of emerging pharmaceutical micropollutants. This work has  
32 assessed the activity and stability of the powder and reticulated porous perovskite (RPP)  
33 material as Fenton-like catalyst. The effect of the initial pH, the temperature and the hydrogen  
34 peroxide were studied using the hospital wastewater fortified with carbamazepine (CZP, 15  
35 mg/L) in order to make easier the evaluation of the catalytic activity in terms of the CZP removal.  
36 The acidification of pH at 3 enhanced the catalytic performance but also increased the leaching  
37 of the constituents of the perovskite material. In contrast, the increase of temperature (from 50  
38 to 90 °C) and hydrogen peroxide dosage (from 350 to 700 mg/L) also improved the performance  
39 of the catalyst, but the stability of the reticulated porous perovskite material hardly was  
40 affected. The catalyst evidenced a remarkable activity (ca. 100 % CZP removal) and stability (low  
41 leaching of the metal species from the  $\text{LaCu}_{0.5}\text{Mn}_{0.5}\text{O}_3$  perovskite) for 70 hours on continuous  
42 operation in a catalytic packed bed reactor operated at 70 °C, initial pH of ca. 5.5 and moderate  
43 dosage of hydrogen peroxide (700 mg/L). Finally, the perovskite catalyst showed a notable  
44 performance for the removal of the pharmaceutical micropollutants detected in the hospital  
45 wastewater in the real range of  $\mu\text{g/L}$  (antineoplastic drugs, antibiotics, X-ray contrast agent,  
46 psychiatric drugs or analgesics & anti-inflammatories). Most of them were eliminated with  
47 removal degrees above 90-95 %. Metoprolol and carbamazepine were the two pharmaceutical  
48 compounds removed in less extension, but in any case, the concentration of both after  
49 treatment was below to the predicted non-effect concentration (PNEC) for aquatic organisms.  
50 Thus, the reticulated porous perovskite material based on  $\text{LaCu}_{0.5}\text{Mn}_{0.5}\text{O}_3$  perovskite is  
51 considered a promising Fenton-like catalyst for its implementation in fixed bed reactors for on-  
52 site pre-treatment of hospital wastewater effluents.

53

54

55

56 **Keywords:** Perovskite, reticulated porous ceramic material, heterogeneous Fenton-like catalyst,  
57 carbamazepine model pollutant, on-site hospital wastewater treatment.

58

## 59 1. INTRODUCTION

60 Nowadays hospital wastewater (HWWs) represent one of the main sources of emerging  
61 pharmaceutical (EP) micropollutants into the environment [1]. HWWs are between 4 and 150  
62 times more concentrated of these EP micropollutants than urban wastewaters (UWWs) [2–4].  
63 However, as the nature of HWWs are similar in nature than UWWs, they are discharged into the  
64 municipal sewer system without any specific pre-treatment [5], and consequently they arrive to  
65 the conventional wastewater treatment plants (WWTPs). Unfortunately, conventional WWTPs  
66 are not able to remove completely the EP micropollutants in most of the cases, and their  
67 effluents become an important source of them in the aquatic ecosystems.

68 Several works have proposed end-of pipe dedicated wastewater treatments for HWWs as a  
69 potential alternative to decrease the load of pharmaceuticals [4]. This has been tested in  
70 different studies over Europe, in which different on-site treatments have been developed for  
71 specific treatment of HWWs, instead of the direct discharge into the municipal sewer system  
72 [5]. In this way, biological treatments based on membrane bioreactors (MBRs) have shown  
73 promising results for the treatment of HWWs with removals of EP micropollutants ranging from  
74 19 to 94 %. These biological processes have been effective for some compounds like  
75 clarithromycin, but others, such as carbamazepine or diclofenac, were hardly removed [6].

76 Alternatively, advanced oxidation processes (AOPs) have been tested as pre-treatment for the  
77 removal of EP micropollutants present in HWWs. Among AOPs, Fenton oxidation has emerged  
78 as a feasible technology for the removal EP micropollutants such as amoxicillin, paracetamol,  
79 ofloxacin, diclofenac, etc. in different waster matrixes [7,8]. Fenton oxidation has been also  
80 proposed for HWWs, but mainly focused on the reduction of the soluble organic matter or the  
81 increase of its biodegradability instead of an efficient removal for EP micropollutants [9,10]. The  
82 main drawbacks of Fenton oxidation are the narrow range of operating pH (2.5-3.5) that is  
83 required for the efficiency of typical soluble catalytic iron species. The use of heterogeneous  
84 Fenton-like catalysts can overcome this limitation as well as the amounts of metallic iron sludge  
85 generated after neutralization and precipitation of the dissolved metallic salts [7,11,12].

86 In this sense, most of heterogeneous Fenton catalysts are based on iron-containing materials  
87 based on the immobilization of iron species in different supports such as zeolites [13], pillared  
88 clays [14], alumina [15], amorphous mesoporous silica [16,17] and activated carbons [18]. But  
89 the use of other low-valency transition-metal ions such as Cu, Mn, Ru, V and Ti may be also  
90 extend the scope of the Fenton reaction [19]. In the last decades, perovskites type oxides have  
91 been extensively investigated as catalysts for several applications [20], including heterogeneous

92 Fenton-like catalyst [21–23]. Perovskite materials are characterized by a crystal structure as  
93  $\text{CaTiO}_3$  and their chemical formula is represented as  $\text{ABO}_3$ , where A-site is a lanthanide metal  
94 (La, Ba, Ca, and Sr) with a 12-coordinated cation and B-site is a transition metal (Ni, Ti, Co, Fe,  
95 Mn or Cu) with a 6-coordinated cation as active site [24]. Their catalytic properties are closely  
96 related to the nature of the A and /or B cations and can be modified by the partial substitution  
97 of A and B, leading to the formation of a variety of mixed oxides. This fact could affect to the  
98 chemical state of the cations, the generation of oxygen vacancies, the mobility of oxygen lattice  
99 and the formation of structural defects [25]. These features make perovskites promising  
100 heterogeneous Fenton-like catalysts.

101 A preliminary work of  $\text{LaCu}_{0.5}\text{Mn}_{0.5}\text{O}_3$  has been reported as an active and stable heterogeneous  
102 Fenton-like catalyst for the removal of paracetamol as model pollutant in ultrapure water [26].  
103 However, the feasibility for real and complex wastewater matrixes, like HWWs, has not been  
104 studied. Moreover, a critical point for the full-scale implementation of powdered heterogeneous  
105 Fenton-type catalysts in fixed-bed reactors and/or stirred tank reactors with stationary catalytic  
106 baskets is that they need to be pelletized or immobilized in opened macrostructures [27,28]. In  
107 this sense, some examples of continuous fixed-bed reactors filled with heterogeneous catalysts  
108 have been proposed to Fenton-like oxidation processes based on packing metallic-based catalyst  
109 pellets [27–31]. In recent years, reticulated porous ceramics (RPCs) have been also investigated  
110 using the polymeric sponge replication method, which is a simple and effective procedure to  
111 make reticulated ceramic foams, also known as open-cell cellular ceramics. In this method, a  
112 porous polymeric sponge used as scaffold is impregnated with a slurry of ceramic precursors to  
113 form a macroporous structure with a high mechanical strength after burning out the organic  
114 polymer and sintering of the ceramic precursors at high temperature [32]. The application of  
115 heterogeneous catalyst conformed as RPCs for AOPs has been hardly reported in literature.  
116 Some examples can be found in photocatalytic systems for water or air purification using RPCs  
117 of different materials (alumina, alumina/mullite, cordierite or polysiloxane-polyurethane foams)  
118 as support of the active  $\text{TiO}_2$  photo catalyst [33–35]. Kocakuşakoğlu et al. demonstrated a  
119 remarkable performance an open three-dimensional network structure of a reticulated porous  
120 ZnO ceramic material with a high interconnected porosity in the photocatalytic degradation of  
121 the azo dye Reactive Red 180 [36].

122 This work will be focused on the preparation of a reticulated porous perovskite (RPP) material  
123 based on  $\text{LaCu}_{0.5}\text{Mn}_{0.5}\text{O}_3$  as heterogeneous Fenton-like catalyst for the removal of emerging  
124 pharmaceutical micropollutants in HWW under continuous operation in a fixed bed reactor. The  
125 RPP material will be prepared following the sponge replication method. The catalytic activity

126 and stability will be assessed at different initial pH values, temperatures and hydrogen peroxide  
127 dosages using a hospital wastewater fortified with carbamazepine (CZP) as model pollutant. CZP  
128 is a common antiepileptic drug with important endocrine disrupting effects in water bodies [37]  
129 which is not effectively removed in wastewater treatment plants [3,6,38]. Finally, the efficiency  
130 of the RPP material will be tested for the removal of the pharmaceutical micropollutants  
131 contained in the hospital wastewater in the real range of concentration of  $\mu\text{g/L}$ .

132

## 133 **2. EXPERIMENTAL**

### 134 **2.1. Materials**

135 The reagents for the synthesis of the powder perovskite material were purchased from Sigma  
136 Aldrich ( $\text{Cu}(\text{CH}_3\text{COO})_2 \cdot 2\text{H}_2\text{O}$ ,  $\text{Mn}(\text{NO}_3)_2 \cdot 4\text{H}_2\text{O}$ ,  $\text{La}(\text{NO}_3)_3 \cdot 6\text{H}_2\text{O}$  and citric acid). Commercial Dolapix  
137 CE 64, Optapix PA 4G, Contraspum KWE and polyurethane foams (PUS) for the preparation of  
138 the reticulated porous perovskite (RPP) material were kindly provided by Zschimmer & Schwarz  
139 España, S.A. Additionally, bentonite and ethanol used in the manufacturing method were  
140 provided by Süd-chemie and Scharlau S.L., respectively. Carbamazepine and sulphuric acid to  
141 adjust the pH of the catalytic experiments were obtained from Sigma-Aldrich.

### 142 **2.2. Preparation and characterization of reticulated porous perovskite materials**

143 **Synthesis of powder  $\text{LaCu}_{0.5}\text{Mn}_{0.5}\text{O}_3$  perovskite.** It was performed using the method described  
144 by Carrasco-Diaz et al. [26]. Typically,  $\text{Cu}(\text{CH}_3\text{COO})_2 \cdot 2\text{H}_2\text{O}$ ,  $\text{Mn}(\text{NO}_3)_2 \cdot 4\text{H}_2\text{O}$  and  $\text{La}(\text{NO}_3)_3 \cdot 6\text{H}_2\text{O}$  as  
145 metallic sources were completely dissolved in 100 mL of ultrapure water. Then, citric acid was  
146 added until achieving a pH of  $2.5 \pm 0.3$ , and the resultant mixture was stirred for 3 h. Thereafter,  
147 the solution was dried at  $70^\circ\text{C}$  for 12 hours to form the sol-gel, and then at  $110^\circ\text{C}$  for 16 hours  
148 to obtain the amorphous solid. After that, it was crushed and sieved until a particle size between  
149 236 and 254 nm, and finally calcined at  $700^\circ\text{C}$  for 5 h in air atmosphere to obtain the powdered  
150  $\text{LaCu}_{0.5}\text{Mn}_{0.5}\text{O}_3$  perovskite material.

151 **Preparation of reticulated porous perovskite material.** It was prepared following the sponge  
152 replica method commonly used for the manufacturing of  $\text{TiO}_2$  and other ceramic foams [32,39].  
153 In this case, the powdered perovskite and additional inorganic binder (bentonite) were  
154 dispersed in ethanol (1 perovskite: 0.25 bentonite: 0.6 ethanol in wt.). Thereafter, a  
155 deflocculating agent (Dolapix CE 64; 65 wt. % respect to perovskite mass) was added to avoid  
156 the agglomeration of the powder particles. After a good dispersion, Optapix RA 4G (polyvinyl  
157 alcohol, 4 wt. % respect to perovskite mass) as organic binder and drops of non-ionic anti-  
158 foaming agent (Contraspum KWE) were added to the slurry suspension. The mixture was

159 maintained under vigorous stirring for 10 minutes. After that, a polyurethane foam of 40 ppi  
160 (pores per linear inch) with a cylindrical form (15 mm-diameter and 40 mm-height) was  
161 immersed in the perovskite-containing slurry suspension. After 30 min, the soaked foam was  
162 taken out and dried for 24 hours at ambient temperature. This procedure was performed twice.  
163 Finally, the organic polymer used as scaffold of the reticulated porous perovskite material was  
164 removed by calcination at 700 °C for 2 hours using a ramp of 5 °C/min and sintered at 1000 and  
165 1200 °C for 2 hours with a heating rate of 5 °C/min.

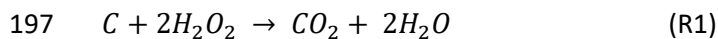
166 **Characterization techniques.** X-ray diffraction (XRD) patterns of powder samples were carried  
167 out in an XPert Pro Diffractometer (Philips PW0340/00) using the CuK $\alpha$  radiation. Data were  
168 recorded at the 2 $\theta$  angle ranging from 10° to 90° with steps of 0.04° and 2 s of accumulation  
169 each step. The composition of the synthesized perovskite material was determined by ICP-AES  
170 using a Vista AX Pro-720ES equipment, being the samples were previously digested under strong  
171 acid medium (HNO<sub>3</sub>/HCl). Mechanical strength under compression of the reticulated porous  
172 perovskite materials was determined using a standardized mechanical test in a dynamometer  
173 Chatillon Force Measurement LTCM Series from AMETEK GmbH, according to ASTM D  
174 4179/2011. In this test, probes of 1 cm<sup>3</sup> are subjected to a controlled compression program until  
175 failure. Finally, porosity of the reticulated samples ( $\epsilon$ ) were determined by the dislodged water  
176 known volume after its immersion in water.

### 177 **2.3. Catalytic performance of perovskite materials for the removal of emerging** 178 **micropollutants in hospital wastewater**

179 **Origin of the hospital wastewater (HWW).** The hospital wastewater was taken directly from the  
180 main collector of a hospital located in the South of Madrid (Spain). In this central collector, three  
181 catch basins discharged their effluents from different activities carried out in the hospital. One  
182 of them correspond to general areas, X- rays and digestive areas. Whereas, the other two are  
183 from laboratories and ICU, anatomic, sterilization and pharmacology. The hospital wastewater  
184 used in this work is a mixture of the three effluents. In order to collect representative samples  
185 of the hospital daily discharge, three automatic auto-samplers of each collector basin were used  
186 to take 330 mL (110 mL each) of wastewater every 10 min through 7 days and mixed together,  
187 collecting up to 1000 L. The wastewater stored at 4 °C showed a COD and TOC concentrations  
188 of 179 mg/L and 130 mg/L, respectively. The nitrogen content was 41 mg/L of N-NH<sub>4</sub><sup>+</sup> and 69  
189 mg/L of Total Kjeldahl Nitrogen (TKN). Finally, the phosphorus content was ca. 3 mg/L P-PO<sub>4</sub><sup>3-</sup>.

190 **Preliminary catalytic tests of the powdered perovskite material.** These experiments were  
191 performed in a stirred tank reactor in batch-wise operation. In a typical experiment, 600 mL of  
192 the HWW was spiked with 15 mg/L of carbamazepine (CZP) and placed in the reactor under

193 continuous stirring (700 rpm). The pH was adjusted, if necessary, by addition of H<sub>2</sub>SO<sub>4</sub> 2 N. Once  
194 the desired temperature was achieved, 0.6 g/L of the powder catalyst and 700 mg/L of H<sub>2</sub>O<sub>2</sub>  
195 (stoichiometric concentration for total TOC consumption according to reaction R1) were added  
196 into the reactor, starting the reaction.



198 The time of each experiment was extended until the hydrogen peroxide was completely  
199 consumed. The temperature (30, 50 and 70 °C) and the pH value (3, 5.5 and 7.5, corresponding  
200 to the natural pH of the HWW) were studied in batch experiments for the powdered perovskite  
201 catalyst.

202 **Catalytic runs of reticulated porous perovskite material.** These experiments were evaluated in  
203 a continuous up-flow fixed bed reactor (FBR) at atmospheric pressure. The FBR consists of a  
204 jacketed cylindrical tube of 1.5 cm of inner diameter and 25 cm of length. The catalytic bed was  
205 formed by 3 g of the reticulated porous perovskite catalyst. Spherical inert glass particles were  
206 located upper and lower to the catalyst bed in order to maintain it stable on place. The hospital  
207 wastewater was pumped by means of a ProMinent GUGAL S.A. pump, model DULCO®flex at 1  
208 mL/min, giving a residence time of 3 minutes, according to equation 1 [40], where  $\varepsilon$  and  $V_{bed}$  are  
209 the porosity and volume of the reticulated porous perovskite material in the FBR.

$$210 \quad t_{R} = \frac{\varepsilon V_{bed}}{Q} \quad (1)$$

211 The temperature of the catalytic runs was controlled using an external heating device of silicon  
212 oil that it is recirculated through the jacket of the reactor. Initially, the HWW was spiked with 15  
213 mg/L of carbamazepine (CZP) and the activity and stability of the reticulated porous perovskite  
214 material in continuous operation was evaluated at different temperatures (50, 70 and 90 °C) and  
215 hydrogen peroxide dosages (700 mg/L and 350 mg/L). Finally, the performance of the catalyst  
216 was assessed for the removal of the emerging pharmaceutical micropollutants of the hospital  
217 wastewater at their real concentration.

218 **Analytical techniques.** Total Organic Carbon (TOC) was determined in a combustion/non-  
219 dispersive infrared gas analyser model TOC-V Shimadzu. Carbamazepine in the range of 0.15-15  
220 mg/L was determined by a HPLC (Varian ProStar) equipped with a Phenomenex C18 (3 x 150  
221 mm) column coupled to a pre-column Phenomenex HPLC Guard Cartridge System using a UV  
222 detector at 254 nm. A solution composed by HPLC quality methanol (49.5 %), ultrapure water  
223 (49.5 %) and glacial acetic acid (1 %) with a final pH value of 2-2.5 was used as mobile phase with  
224 a flowrate of 0.30 mL/min. Hydrogen peroxide was determined by a colorimetric method (DEV

225 (H15)) according to DIN 38 409 based on the measurement of the chromophore formed at 410  
226 nm after the addition of a standard commercial solution of titanium oxysulfate ( $\text{TiOSO}_4$  1.9-2.1  
227 %). The concentration of dissolved metals from the perovskite after treatment in the aqueous  
228 samples were measured by ICP-AES (Varian, Vista AX Pro-720ES). The emerging pharmaceutical  
229 micropollutants detected in the hospital wastewater and samples after treatment were  
230 analysed by ultra-high-performance liquid chromatography-tandem mass spectrometry  
231 (UHPLC-ESI-MS/MS) using vortex electrospray ionization interface (Bruker UHPLC/MSMS  
232 EVOQ™ QUBE). The method includes 22 pharmaceutical micropollutants of 7 different  
233 therapeutic groups (Table 1\_SM). The samples were filtered through a dura-pore hydrophilic  
234 filter (PVDF, 0.65  $\mu\text{m}$ ) and extracted by solid phase extraction (SPE) using a polymeric cartridge  
235 (TELOS C18(EC), 200 mg/6 mL) from Kinesis. Chromatographic separation was achieved with a  
236 Bruker Intensity Solo 2 C18 column (100 x 2.1 mm and 2 $\mu\text{m}$ ). The mobile phase (flow rate 400  
237  $\mu\text{L}/\text{min}$ ) consisted of a gradient program of water with 0.04 % acetic acid and acetonitrile at 40  
238 °C [41].

239

### 240 **3. RESULTS AND DISCUSSION**

#### 241 **3.1. Preparation and characterization of the reticulated porous perovskite catalyst**

242 According to the method used for the preparation of the reticulated porous ceramics, several  
243 preliminary experiments were needed to determine the optimal composition of the slurry  
244 suspension for a successful conformation of the final reticulated porous perovskite material. In  
245 these experiments, the dosage of bentonite and Optapix PA 4G as inorganic and organic binders  
246 was carefully studied in order to find an optimal viscosity of the slurry suspension for a complete  
247 soaking of the macroporous structure of the polyurethane sponge. Experimentally, it was  
248 determined that amounts of 25 wt. % (bentonite) and 4 wt. % (Optapix PA 4G) in basis to the  
249 mass of powdered perovskite, enables a good penetration of the slurry solution into the sponge  
250 structure to form final stable reticulated porous materials after removal of the organic polymer  
251 scaffold by calcination.

252 After optimization of the binders' composition of the slurry suspension that contains the active  
253 perovskite material for the dip-coating of a polyurethane sponge, the slow removal of the  
254 organic skeleton by calcination with a controlled heating rate is a key variable for obtaining a  
255 consistent reticulated porous material. According to the thermogravimetric analysis of the  
256 polyurethane sponge (Figure 1\_SM), a temperature of 700 °C and a heating rate of 2.5 °C/min  
257 was established for achieving a slow and complete decomposition of the organic polyurethane.  
258 Likewise, a further thermal treatment for sintering of the reticulated porous material was



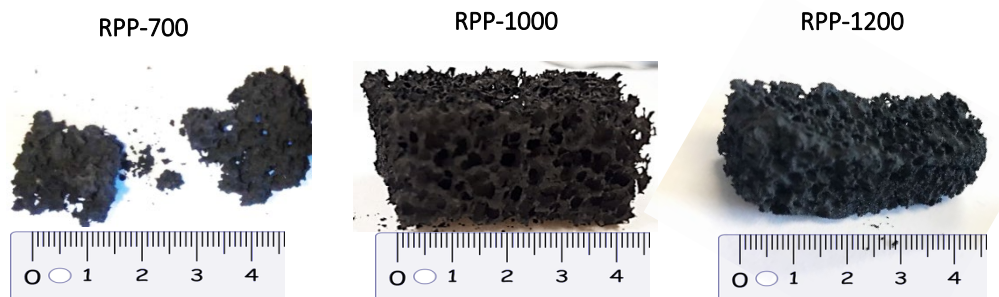
259 studied at 1000 and 1200 °C. Table 1 shows the porosity ( $\epsilon$ ) and the mechanical strength of the  
 260 reticulated porous perovskite (RPP) materials after primary calcination at 700 °C and secondary  
 261 calcination at 1000 and 1200 °C. At 1000 °C, a stable reticulated porous perovskite material was  
 262 achieved with a mechanical strength of 14 N and porosity of 0.6. The increasing of temperature  
 263 up to 1200 °C enhances the mechanical strength until 23 N, but the porosity significantly  
 264 decreased to 0.3, probably due to the shrinkage and partial collapsing of the perovskite-based  
 265 structure with the temperature. On the other hand, it was clearly evidenced that 700 °C was  
 266 insufficient to obtain a reticulated porous material consistent enough. Figure 1 shows images of  
 267 RPP materials calcined at 700, 1000 and 1200 °C.

268

269 **Table 1.** Properties of  $\text{LaCu}_{0.5}\text{Mn}_{0.5}\text{O}_3$ -RPPs prepared with different sintering temperatures.

Sample	$T_{\text{final}}$ (°C)	$\epsilon$	Resistance (N)
RPP-700	700	Non-stable structure	
RPP-1000	1000	0.60	$14 \pm 3$
RPP-1200	1200	0.30	$23 \pm 3$

270

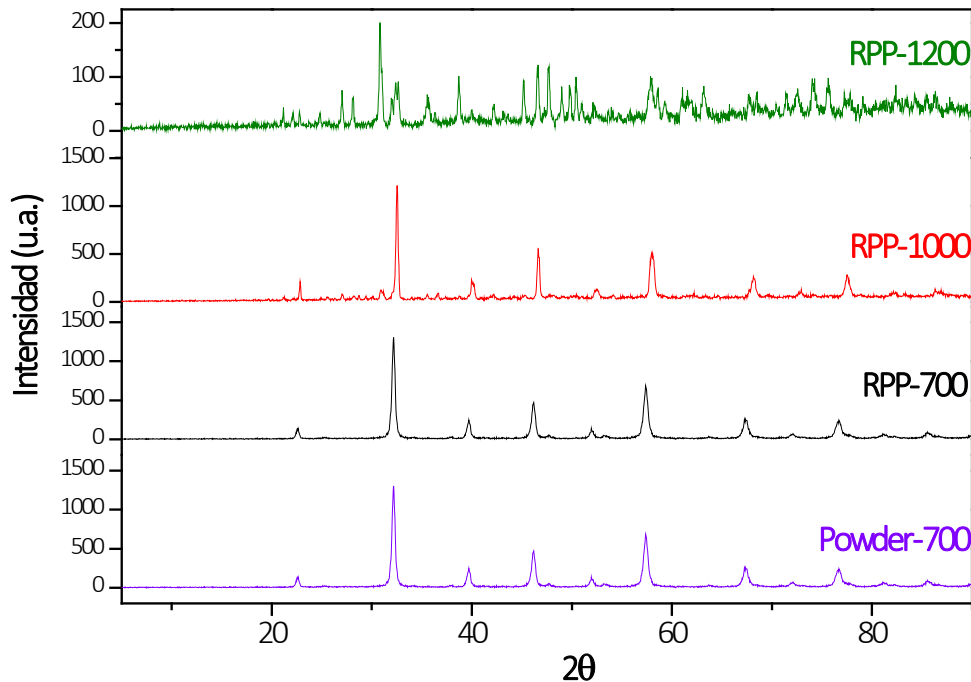


271 **Figure 1.** Images of calcined reticulated porous perovskite materials at 700, 1000 and 1200 °C

272

273 Additionally, XRD patterns of powder reticulated porous materials after crushing (RPP-700, RPP-  
 274 1000 and RPP-1200) were assessed as compared to the powder  $\text{LaCu}_{0.5}\text{Mn}_{0.5}\text{O}_3$  perovskite  
 275 precursor (Figure 2). The RPP-700 material showed characteristic diffraction peaks at 22.6°,  
 276 32.2°, 39.8°, 46.2° and 57.4°, corresponding to (101), (121), (220), (202) and (240) lattice planes  
 277 of the standard  $\text{ABO}_3$  structure (JCPDS file: 37-1493). The RPP-1000 material retains the typical  
 278  $\text{ABO}_3$  perovskite structure, although small diffraction peaks at 30 ° appeared, being attributed  
 279 to the presence of bentonite. In the case of RPP-1200 material, the intensity of characteristic

280 signals of ABO<sub>3</sub> perovskite structure decreased and additional diffraction peaks were observed,  
281 which can be attributed to segregation of bentonite (montmorillonite, 28°- 30°), copper oxides  
282 (~35°) and manganese and lanthanum oxides (~43°-47°). These results evidenced a partial  
283 conversion of the perovskite structure to other crystalline phases at 1200 °C.



284 **Figure 2.** XRD patterns of RPP materials and powder LaCu<sub>0.5</sub>Mn<sub>0.5</sub>O<sub>3</sub> perovskite precursor

285

### 286 **3.2. Preliminary catalytic tests of powder LaCu<sub>0.5</sub>Mn<sub>0.5</sub>O<sub>3</sub> perovskite material.**

287 The influence of the initial pH (3, 5.5, 7.5) and temperature (30, 50 and 70 °C) was initially studied  
288 for the treatment of the hospital wastewater spiked with carbamazepine (CZP) as model  
289 pollutant for a better evaluation of the catalytic performance of the powder LaCu<sub>0.5</sub>Mn<sub>0.5</sub>O<sub>3</sub>  
290 perovskite.

291 Figure 3 a and 3 b shows the H<sub>2</sub>O<sub>2</sub> conversion and CZP removal of the catalytic tests carried out  
292 at the initial pH of ca. 7.5 (natural pH of the hospital wastewater) and 30, 50 or 70 °C. The rate  
293 of the oxidant conversion increases with the temperature, achieving a complete conversion at  
294 220 min, 180 min and 120 min for 30, 50 and 70 °C, respectively. Likewise, the removal rates of  
295 CZP are significantly increased with the reaction temperature, reaching removals of 5 %, 75 %  
296 and 100 % at the end of each catalytic run at 30, 50 and 70 °C, respectively. The low efficiency  
297 of the catalyst at 30 °C could be attributed to a predominance of the ineffective decomposition  
298 of H<sub>2</sub>O<sub>2</sub> in H<sub>2</sub>O and ½ O<sub>2</sub> promoted by the oxygen vacancies of the perovskite structure [42]. In

299 fact, the chemical composition of the synthesized powder perovskite ( $\text{LaCu}_{0.5}\text{Mn}_{0.49}\text{O}_{2.79}$ )  
300 evidence a slight defect of oxygen in comparison to the theoretical one ( $\text{LaCu}_{0.5}\text{Mn}_{0.5}\text{O}_3$ ). Blank  
301 experiments performed at 70 °C to determine the oxidative capacity of hydrogen peroxide in  
302 absence of catalyst and the adsorption capacity of perovskite in absence of oxidant (Figure 2\_SM  
303 a and b, respectively), also revealed a low removal of CZP (25 %) by the action of  $\text{H}_2\text{O}_2$  and a  
304 negligible adsorption of CZP. Concerning the TOC mineralization, a low TOC reduction was  
305 observed for all the studied temperatures in the catalytic experiments at the initial pH of 7.5.  
306 The complex composition of the HWW, accompanied with a relevant amount of urea, can be  
307 responsible for this low TOC mineralization [10]. The effect of the complex matrix was confirmed  
308 by repeating the catalytic test at 70 °C with CZP in ultrapure water instead of the hospital  
309 wastewater matrix (Figure 3\_SM). In this case, a remarkable TOC mineralization of ca. 40 % was  
310 achieved after 120 min. The stability of the metallic species of the  $\text{LaCu}_{0.5}\text{Mn}_{0.5}\text{O}_3$  during the  
311 catalytic runs determined by the analysis of the metal ions dissolved in the reaction medium  
312 after reaction (Table 2), evidenced a negligible leaching of metallic species, with values of La and  
313 Mn concentrations below the detection limit (< 0.2 mg/L) and lower than 0.7 mg/L for Cu (less  
314 than 1 % of the Cu content of the solid catalyst).

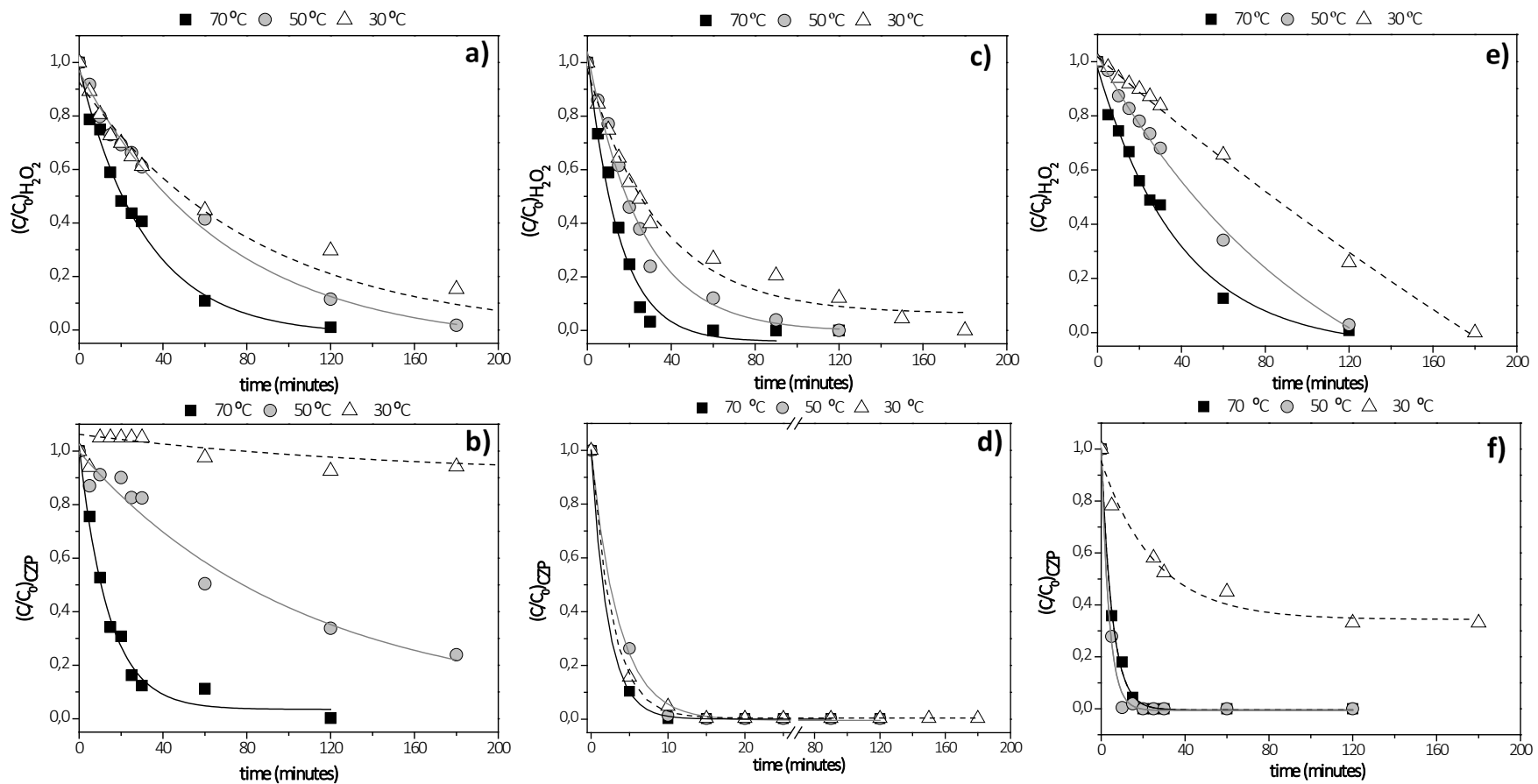
315 The acidification of the initial pH of hospital wastewater up to 3 showed a significant increase of  
316 the conversion of hydrogen peroxide and the removal of CZP even at 30 °C (Figure 3 c and 3 d).  
317 Thus, a complete elimination of CZP was reached in less than 20 minutes at this temperature,  
318 being necessary less than 10 minutes at 50 and 70 °C. These results reveal a better efficiency of  
319 the oxidant, which is attributed to the higher oxidation potential of hydroxyl radicals at acid pH  
320 (2.7 V at pH 3 vs. 1.8 V at pH 7) [43]. The TOC removal was also improved at this pH, achieving  
321 values of ca. 19, 31 and 36 % for 30, 50 and 70 °C, respectively. However, it must be noteworthy  
322 that the metal leaching of the perovskite catalyst dramatically increased with the acid pH,  
323 obtaining concentrations of La, Cu and Mn after reaction between 87-113, 18-22 and 20-25  
324 mg/L, respectively (Table 2). Thus, the acidification of pH at 3 significantly affects the stability of  
325 the  $\text{LaCu}_{0.5}\text{Mn}_{0.5}\text{O}_3$  perovskite material, limiting its application as Fenton-like catalyst.

326 Catalytic experiments at pH of 5.5 (Figure 3 e and 3 f) also revealed a good catalytic performance  
327 of  $\text{LaCu}_{0.5}\text{Mn}_{0.5}\text{O}_3$  perovskite with remarkable conversions of hydrogen peroxide and removal  
328 rates of carbamazepine. CZP removals higher than 95 % were achieved in less than 10 minutes  
329 at 50 and 70 °C. At 30 °C, the removal of CZP was significantly higher than that obtained at the  
330 pH of 7.5, but still low with only 65 % of removal after 180 min of reaction. Thus, a minimum  
331 temperature of 50 °C seems to be recommendable for a fast CZP degradation. Regarding the  
332 catalyst stability, the metal concentration of La, Cu and Mn after reaction were in the range of

333 0.6-1.1, 1.2-1.3 and 1.2-3.7 mg/L, respectively (Table 2). These concentrations correspond to  
334 percentages of metal leaching lower than 6 % in all the cases. Moreover, it was observed that  
335 the catalyst stability is not significantly depended on the reaction temperature in the studied  
336 interval (30 - 70 °C). These results of the metal leaching demonstrate a higher stability of the Cu  
337 on the solid catalyst as compared to that obtained by other copper-containing catalysts  
338 operating in analogous reaction conditions, making  $\text{LaCu}_{0.5}\text{Mn}_{0.5}\text{O}_3$  perovskite a promising  
339 heterogeneous Fenton-like catalyst [23,44,45].

340 Summarizing, the performance of  $\text{LaCu}_{0.5}\text{Mn}_{0.5}\text{O}_3$  perovskite in terms of the CZP removal  
341 progressively increased with the decrease of pH, but in detriment of catalyst stability. The better  
342 compromise between activity and stability is obtained at pH values and temperatures equal or  
343 higher than 5.5 and 50 °C, respectively. This pH is the minimum value in which the lixiviation of  
344 metallic species and consequently the loss of active phase is still negligible. At the same time,  
345 50 °C was the minimum temperature required in order to obtain a desirable catalyst activity in  
346 terms of CZP removal, hydrogen peroxide consumption and TOC mineralization. At 50 °C and  
347 initial pH of 5.5, it was reached a total CZP removal in hardly 10 minutes and a TOC mineralization  
348 of ca. 22 % after 120 min. Moreover, these results are obtained using a catalyst loading (0.6 g/L)  
349 and hydrogen peroxide concentration (0.7 g/L), amounts that are much lower than those used  
350 in other works reported in literature for the elimination of CZP through homogeneous and  
351 heterogeneous Fenton processes. So, Sun et al. hardly achieved a 3 % removal of a 15 mg/L  
352 solution of CZP after 180 min of reaction, using 5 mg/L of a homogeneous Fe(III) catalyst at  
353 neutral pH, room temperature and 0.6 g/L of  $\text{H}_2\text{O}_2$  [46]. The use of a heterogeneous catalyst of  
354  $\text{Fe}_3\text{O}_4$  nanoparticles with a concentration of 1.84 g/L and 20 g/L of  $\text{H}_2\text{O}_2$  achieved a CZP removal  
355 of 86 % at neutral pH and room temperature [47]. However, a decrease of the catalyst loading  
356 and the oxidant concentration up to 1 g/L and 3.4 g/L, respectively, dramatically reduced the  
357 effectivity of the catalyst, leading to a removal of CZP of only 6 %.  $\text{CuFeO}_2$  micro-particles  
358 achieved a 31 % removal of CZP in 60 minutes at room temperature and neutral pH, but needing  
359 a  $\text{H}_2\text{O}_2$  concentration and a catalyst loading of 7 g/L and 1 g/L respectively [48].

360



361 **Figure 3.** Normalized concentration of hydrogen peroxide and carbamazepine concentrations at initial pH of 7.5 (a) and (b), 3 (c) and (d), 5.5 (e) and (f) for  
 362 different reaction temperatures (30, 50, and 70 °C) in batch experiments with powder  $LaCu_{0.5}Mn_{0.5}O_3$  perovskite at:  $[H_2O_2]_0 = 700$  mg/L,  $[catalyst] = 0.6$  g/L,  
 363  $[CZP]_{spiked} = 15$  mg/L in HWW and stirring =700 rpm

364 **Table 2.** Metal leaching of catalytic tests performed at different temperatures and initial pH  
 365 values using  $\text{LaCu}_{0.5}\text{Mn}_{0.5}\text{O}_3$ . Values in brackets correspond to percentage of metal lost from the  
 366 solid catalyst

pH	T (°C)	[La]	[Cu]	[Mn]
		(mg/L)		
7.5	70	< 0.2 (0.06 %)	$0.37 \pm 0.06$ (0.5 %)	< 0.2 (0.3 %)
	50	< 0.2 (0.06 %)	$0.48 \pm 0.07$ (0.6 %)	< 0.2 (0.3 %)
	30	< 0.2 (0.06 %)	$0.67 \pm 0.06$ (0.9 %)	< 0.2 (0.3 %)
5.5	70	$0.60 \pm 0.02$ (0.2 %)	$1.24 \pm 0.90$ (1.3 %)	$1.39 \pm 0.09$ (2.1 %)
	50	$1.10 \pm 0.03$ (0.3 %)	$1.57 \pm 0.91$ (2 %)	$3.66 \pm 0.07$ (5.5 %)
	30	$0.97 \pm 0.03$ (0.3 %)	$1.27 \pm 0.90$ (1.6 %)	$1.11 \pm 0.10$ (1.7 %)
3	70	$94 \pm 1$ (28 %)	$19 \pm 1$ (25 %)	$21 \pm 1$ (31 %)
	50	$113 \pm 3$ (33 %)	$22 \pm 1$ (28 %)	$25 \pm 1$ (37 %)
	30	$87 \pm 1$ (26 %)	$18 \pm 1$ (23 %)	$20 \pm 1$ (30 %)

367

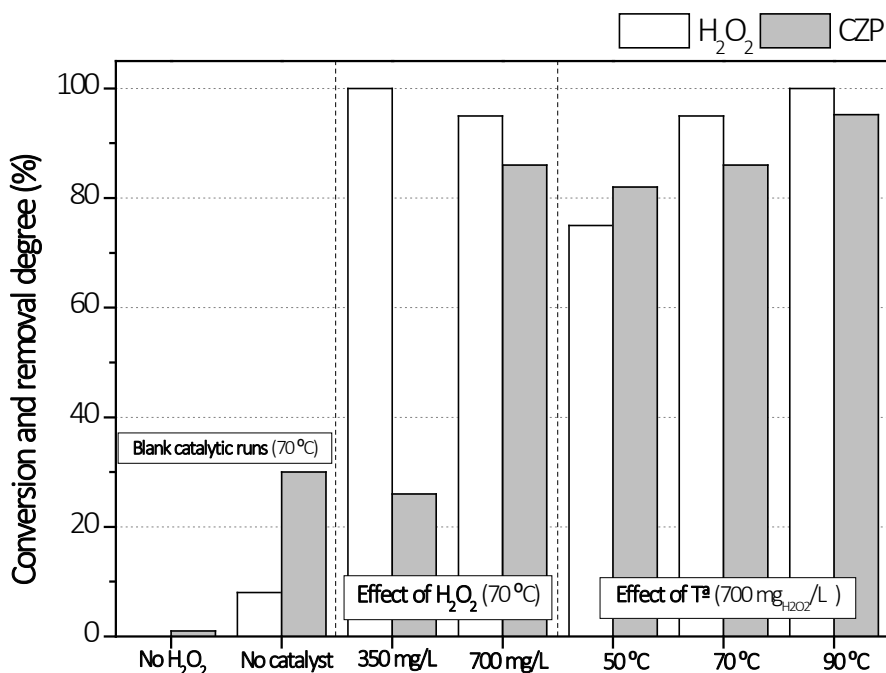
368

369 **3.3. Catalytic performance of reticulated porous perovskite materials in continuous up-flow**  
 370 **fixed bed reactor**

371 The two reticulated porous perovskite materials RPP-1000 and RPP-1200 were tested in a  
 372 catalytic fixed bed reactor for the treatment of the HWW spiked with 15 mg/L of CZP. These  
 373 catalytic runs were performed at 70 °C, initial pH of 5.5, stoichiometric dosage of hydrogen  
 374 peroxide (700 mg/L) and residence time of 3 min. The RPP-1200 was less active than RPP-1000  
 375 with a  $\text{H}_2\text{O}_2$  conversion and CZP removal of ca. 20 and 70 %, respectively. On the contrary, the  
 376 RPP-1000 achieved a total consumption of the oxidant and CZP removal higher than 90 %. The  
 377 oxidant conversion and CZP removal of both experiments along the time on operation at steady-  
 378 state conditions can be found in Figure 4\_SM. The lower catalytic performance of RPP-1200  
 379 material is attributed to the loss of the perovskite active phase and porosity when the material  
 380 was calcined at 1200 °C for sintering of the reticulated porous material. On the other hand, it  
 381 was very remarkable that both materials maintained their physical reticulated porous structure

382 after 5 hours on operation. Moreover, the leaching of the metal containing in the perovskite  
383 catalyst was almost negligible.

384 In order to assess the influence of the temperature in continuous operation of the up-flow fixed  
385 bed reactor using the reticulated porous perovskite material RPP-1000, additional catalytic runs  
386 were carried out at 50 and 90 °C. These experiments were performed maintaining the  
387 acidification of the hospital wastewater up to 5.5, the stoichiometric amount of H<sub>2</sub>O<sub>2</sub> (700 mg/L)  
388 and the residence time at 3 min. Figure 4 shows the hydrogen peroxide conversion and the CZP  
389 removal at steady-state conditions after 5 hours of continuous operation at 50, 70 and 90 °C. At  
390 50 °C, 82 % of CZP was eliminated but not all the hydrogen peroxide was used (74 % of oxidant  
391 conversion). The increase of temperature up to 90 °C allows a total oxidant conversion with the  
392 increase of the CZP removal until 92 %. It must be noted that the stability of the reticulated  
393 porous perovskite material was not significantly affected by the increase of temperature, with  
394 concentrations of La, Cu and Mn in the outlet effluent ranging from 0.2-3.8 mg/L, 1.0-2.3 and  
395 3.2-5.9, respectively. The overall metal leaching from the solid catalyst after 5 hours of operation  
396 was in all the cases lower than 8 %. These results indicate a high stability of the reticulated  
397 porous perovskite catalysts. Additionally, the initial H<sub>2</sub>O<sub>2</sub> concentration was decreased from 700  
398 to 350 mg/L at 70 °C in order to evaluate the performance of the RPP-1000 material at a lower  
399 oxidant dosage (Figure 4). It must be noted that the hydrogen peroxide is the most significant  
400 cost in Fenton operation process. The removal of carbamazepine significantly decreases at  
401 steady state (after 5 hours of operation) from 87 % to 40 %. Additional catalytic run in absence  
402 of hydrogen peroxide evidenced a negligible CZP removal (see Figure 4). These results indicates  
403 the important role of the oxidant in the production of hydroxyl radicals and consequently the  
404 oxidation of carbamazepine [49]. Thus, the catalytic performance is enhanced by the  
405 temperature and the catalyst was very stable even at 90 °C. The intermediate temperature of  
406 70 °C allowed a remarkable CZP removal (ca. 87 %) with an almost total oxidant conversion (93  
407 %). Moreover, the results of a non-catalytic run with only hydrogen peroxide proved the active  
408 role of the catalyst. The run performed in absence of catalyst (RPP-1000 replaced by equivalent  
409 volume of glassy spheres of 1 mm diameter) achieved only a 30 % of CZP removal by the  
410 potential oxidation of hydrogen peroxide (Figure 4). The H<sub>2</sub>O<sub>2</sub> conversion and CZP removal of  
411 the catalytic runs performed at different temperatures and hydrogen peroxide dosages along  
412 the time on operation are shown in Figure 5\_SM and 6\_SM, respectively.

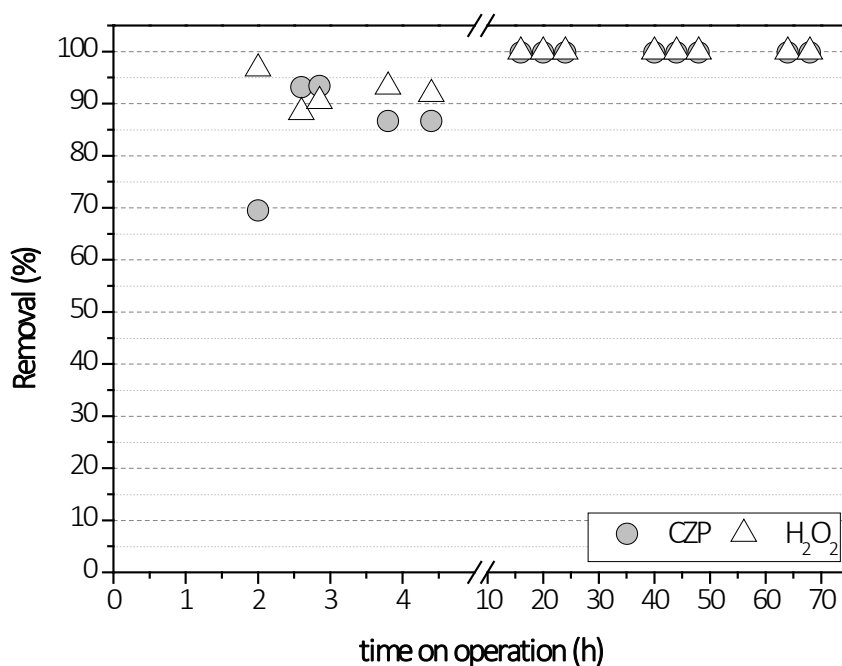


413 **Figure 4.** Influence of temperature and hydrogen peroxide dosage on the catalytic performance  
 414 of reticulated porous perovskite material RPP-1000 in a catalytic fixed bed reactor. Operation  
 415 conditions: HWW spiked with CZP (15 mg/L), acidification at pH of 5.5, residence time = 3 min.  
 416

417 Few works have approached the study of continuous Fenton processes using heterogeneous  
 418 catalytic systems for long periods of operation [50,51]. Iron nanoparticles embedded within  
 419 ordered mesoporous carbon catalyst (Fe-OMC) showed a phenol conversion above 90 %,   
 420 although the efficiency decreased during 39 h of long-term evaluation [50]. A Highly dispersed  
 421 Fe<sup>3+</sup>-Al<sub>2</sub>O<sub>3</sub> catalyst (6 wt. % Fe) retained remarkable mineralization levels of phenol ( $X_{TOC} > 70\%$ )  
 422 with a cumulative iron loss of ca. 20 % of the initial Fe loaded in an up-flow fixed bed reactor  
 423 (UFBR) after 70 hours on operation [51]. In this work, the catalytic performance of reticulated  
 424 porous perovskite catalyst was tested for 70 hours at 70 °C, slight acid pH (5.5) and moderate  
 425 hydrogen peroxide concentration (700 mg/L) in order to assess the feasibility of the catalyst for  
 426 long-term continuous treatment of the hospital wastewater. Figure 5 shows the results of  
 427 oxidant conversion and CZP removal along the time on operation. Interestingly, the CZP  
 428 elimination increases up to complete removal after 10 h on operation accompanied with a total  
 429 hydrogen peroxide conversion. Moreover, the reticulated porous perovskite material keeps  
 430 constant a total CZP removal and hydrogen peroxide conversion and maintains its mechanical  
 431 integrity up to 70 h on operation. The TOC reduction was of hardly 10 % at steady-state



432 conditions, as consequence of the refractory behaviour of the complex HWW matrix. Therefore,  
 433 this catalytic system is proposed as an alternative on-site pre-treatment for the removal of  
 434 pharmaceutical micropollutants, prior to discharge of the HWW into the sewer system for final  
 435 depuration of the water in a conventional WWTP [5]. These results make this reticulated porous  
 436 perovskite catalyst a promising catalyst to be applied in continuous Fenton processes based on  
 437 fixed bed reactors, in this case for the removal of pharmaceutical micropollutants in hospital  
 438 wastewaters.



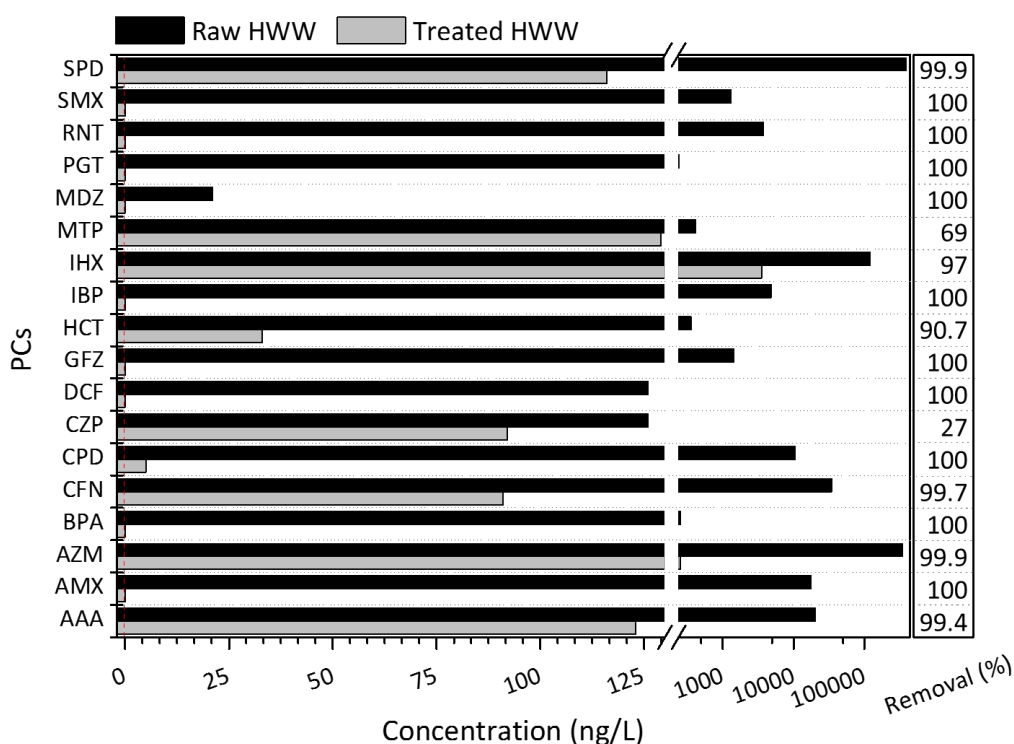
439 **Figure 5.** Long term catalytic run of reticulated porous perovskite material RPP-1000 in a  
 440 catalytic fixed bed reactor. Operation conditions: HWW spiked with CZP (15 mg/L), acidification  
 441 at pH of 5.5, 70 °C, [H<sub>2</sub>O<sub>2</sub>] = 700 mg/L and residence time = 3 min.

442

443 **3.4. Catalytic performance of reticulated porous perovskite material for the removal of**  
 444 **emerging pharmaceutical micropollutants of hospital wastewater**

445 The removal of the pharmaceutical micropollutants contained in the HWW at their original  
 446 concentration was evaluated. In this case, additional carbamazepine was not spiked in the  
 447 HWW. Figure 6 shows the concentration of the pharmaceutical micropollutants before and after  
 448 the treatment and the removal efficiency using the reticulated porous perovskite material RPP-  
 449 1000 in the fixed bed reactor. Eighteen pharmaceutical micropollutants were detected in the  
 450 hospital wastewater (Table 1\_SM). Antypirine (AAA), amoxicillin (AMZ), caffeine (CFN),

451 azithromycin (AZM), cyclophosphamide (CPD), iohexol (IHX) and sulpiride (SPD) were the most  
452 abundant compounds with concentrations ranging from 10 to 390 µg/L. These drugs are  
453 commonly used in hospitals as analgesic/anti-inflammatory, antibiotic, stimulating,  
454 antineoplastic, X-ray agent and psychiatric drugs. Gemfibrozil (GFZ), ibuprofen (IBU), ranitidine  
455 (RNT) and sulfamethoxazole (SMX) as lipid regulator, anti-inflammatory, antagonist receptor  
456 and antibiotic, respectively, were found in concentrations from 1 to 10 µg/L. The rest of  
457 compounds including bisphenol A (BPA), carbamazepine (CZP), diclofenac (DCF),  
458 hydrochlorothiazide (HCT), metoprolol (MTP), metrodinazole (MDZ) and progesterone (PGT),  
459 were detected in much lower concentrations (< 1 µg/L). The presence and concentrations of  
460 these pharmaceutical micropollutants in the HWW are in accordance to the typical  
461 characterization of these effluents with analgesics, antibiotics and contrast agents as some of  
462 the main contributing therapeutic groups [52]. The catalyst was extremely efficient for the  
463 removal of 9 micropollutants with concentrations after treatment below the detection limits. All  
464 the most abundant compounds (CFN, CPD, AZM, IHX, SPD, AMX and AAA) were eliminated with  
465 efficiencies above 95 % and 90 % for the case of HCT. Only two compounds detected at very low  
466 concentrations such as metropolol (MTP,  $0.42 \pm 0.45$  µg/L) and carbamazepine (CZP,  $0.13 \pm 0.01$   
467 µg/L) showed lower removal degrees. The low removal efficiency of these two micropollutants  
468 can be due to the lower efficiency of hydroxyl radicals for oxidizing more diluted concentration.  
469 Moreover, very low concentrations are more susceptible to sampling and analytical error [53].  
470 Nevertheless, it must be noted that the remaining CZP and MTP concentrations (ca. 0.09 µg/L  
471 and 0.13 µg/L, respectively) are quite lower than their predicted non-effect concentration  
472 (PNEC) (2.5 µg/L and 7.9 µg/L, for CZP and MTP, Table 1\_SM). It also occurs for the remaining  
473 PCs' concentrations in the treated HWW (Table 1\_SM), demonstrating that the risk for aquatic  
474 organisms can be ruled out after this Fenton heterogeneous treatment.



476 **Figure 6.** Concentration of pharmaceutical micropollutants in the raw and treated HWW after  
 477 the Fenton treatment in the FBR and removal efficiencies achieving for each PC. Reaction  
 478 conditions:  $T = 70\text{ }^{\circ}\text{C}$ ,  $\text{pH} = 5.5$ ,  $[\text{H}_2\text{O}_2]_0 = 700\text{ mg/L}$ ,  $\text{LaCu}_{0.5}\text{Mn}_{0.5}\text{O}_3\text{-RPC} = 3\text{ g} = 3\text{ g}$  and flow rate  
 479  $= 1\text{ mL/min}$  ( $t_R = 3\text{ min}$ ).

480

#### 481 4. CONCLUSIONS

482 Powdered  $\text{LaCu}_{0.5}\text{Mn}_{0.5}\text{O}_3$  perovskite was successfully immobilized on a reticulated porous  
 483 structure by double impregnation and calcination at  $1000\text{ }^{\circ}\text{C}$ , achieving a high mechanical  
 484 resistance and non-alteration of its characteristic  $\text{ABO}_3$  lattice. The activity and stability of  
 485  $\text{LaCu}_{0.5}\text{Mn}_{0.5}\text{O}_3$  perovskite as heterogeneous Fenton-like catalyst was tested for the removal of  
 486 carbamazepine spiked in a hospital wastewater matrix as model pollutant. The powdered  
 487  $\text{LaCu}_{0.5}\text{Mn}_{0.5}\text{O}_3$  perovskite showed a complete CZP removal (120 minutes) and low values of  
 488 metal leaching ( $< 1\text{ mg/L}$ ) at the natural pH of the wastewater (7.5) and  $70\text{ }^{\circ}\text{C}$ . At pH of 3, the  
 489 stability of the perovskite dramatically decreased. The acidification until pH of 5.5 allows a  
 490 complete CZP removal in 20 minutes with a remarkable enhancement of the stability. The  
 491 reticulated porous perovskite catalyst has achieved a complete removal of CZP at steady-state  
 492 conditions in an up-flow fixed bed reactor for the continuous treatment of a wastewater fortified  
 493 with CZP at weak acid pH (5.5),  $70\text{ }^{\circ}\text{C}$  and moderate dosage of hydrogen peroxide (700 mg/L).

494 This catalyst maintained its mechanical integrity and catalytic activity for 70 hours on operation.  
495 Likewise, the most abundant compounds (CFN, CPD, AZM, IHX, SPD, AMX and 4-AAA) of the  
496 hospital wastewater at the real concentrations of  $\mu\text{g/L}$  were eliminated with high efficiencies  
497 between 95 and 100 %. Only some compounds detected at the lowest concentrations ( $< 1 \mu\text{g/L}$ )  
498 showed lower removal degrees. The catalytic activity and the low leaching of the reticulated  
499 porous  $\text{LaCu}_{0.5}\text{Mn}_{0.5}\text{O}_3$  perovskite for operation at weak acid pH makes this material a promising  
500 catalyst for application in Fenton-like processes using up-flow fixed bed reactors.

501

## 502 **ACKNOWLEDGEMENTS**

503 The authors thank the financial support by the Comunidad de Madrid and FEDER program (EU)  
504 through the projects S2013/MAE-2716 and S2018/EMT-4341. Authors also thanks *Zschimmer &*  
505 *Schwartz ES*, for supplying for free *Dolapix CE 64*, *Contraspum KWE* and *Octapix RA 4G* for the  
506 preparation of the reticulated porous perovskite structures.

507

## 508 **REFERENCES**

- 509 [1] E.A. Serna-Galvis, J. Silva-Agreto, A.M. Botero-Coy, A. Moncayo-Lasso, F. Hernández, R.A.  
510 Torres-Palma, Effective elimination of fifteen relevant pharmaceuticals in hospital  
511 wastewater from Colombia by combination of a biological system with a sonochemical  
512 process, *Sci. Total Environ.* 670 (2019) 623–632. doi:10.1016/J.SCITOTENV.2019.03.153.
- 513 [2] P. Verlicchi, M. Al Aukidy, A. Galletti, M. Petrovic, D. Barceló, Hospital effluent:  
514 Investigation of the concentrations and distribution of pharmaceuticals and  
515 environmental risk assessment, *Sci. Total Environ.* 430 (2012) 109–118.  
516 doi:10.1016/J.SCITOTENV.2012.04.055.
- 517 [3] T. Chonova, F. Keck, J. Labanowski, B. Montuelle, F. Rimet, A. Bouchez, Separate  
518 treatment of hospital and urban wastewaters: A real scale comparison of effluents and  
519 their effect on microbial communities, *Sci. Total Environ.* 542 (2016) 965–975.  
520 doi:10.1016/J.SCITOTENV.2015.10.161.
- 521 [4] B.I. Escher, R. Baumgartner, M. Koller, K. Treyer, J. Lienert, C.S. McArdell, Environmental  
522 toxicology and risk assessment of pharmaceuticals from hospital wastewater, *Water Res.*  
523 45 (2011) 75–92. doi:10.1016/J.WATRES.2010.08.019.
- 524 [5] P. Verlicchi, M. Al Aukidy, E. Zambello, What have we learned from worldwide  
525 experiences on the management and treatment of hospital effluent? — An overview and

- 526 a discussion on perspectives, *Sci. Total Environ.* 514 (2015) 467–491.  
527 doi:<http://dx.doi.org/10.1016/j.scitotenv.2015.02.020>.
- 528 [6] S. Beier, C. Cramer, S. Köster, C. Mauer, L. Palmowski, H.F. Schröder, J. Pinnekamp, Full  
529 scale membrane bioreactor treatment of hospital wastewater as forerunner for hot-spot  
530 wastewater treatment solutions in high density urban areas, *Water Sci. Technol.* 63  
531 (2011) 66–71. doi:10.2166/wst.2011.010.
- 532 [7] A. Mirzaei, Z. Chen, F. Haghghat, L. Yerushalmi, Removal of pharmaceuticals from water  
533 by homo/heterogenous Fenton-type processes – A review, *Chemosphere.* 174 (2017)  
534 665–688. doi:10.1016/J.CHEMOSPHERE.2017.02.019.
- 535 [8] M.L. Wilde, M. Schneider, K. Kümmerer, Fenton process on single and mixture  
536 components of phenothiazine pharmaceuticals: Assessment of intermediaries, fate, and  
537 preliminary ecotoxicity, *Sci. Total Environ.* 583 (2017) 36–52.  
538 doi:10.1016/J.SCITOTENV.2016.12.184.
- 539 [9] P. Kajitvichyanukul, N. Suntronvipart, Evaluation of biodegradability and oxidation  
540 degree of hospital wastewater using photo-Fenton process as the pretreatment method,  
541 *J. Hazard. Mater.* 138 (2006) 384–391. doi:10.1016/J.JHAZMAT.2006.05.064.
- 542 [10] M. Munoz, P. Garcia-Muñoz, G. Pliego, Z.M. de Pedro, J.A. Zazo, J.A. Casas, J.J. Rodriguez,  
543 Application of intensified Fenton oxidation to the treatment of hospital wastewater:  
544 Kinetics, ecotoxicity and disinfection, *J. Environ. Chem. Eng.* 4 (2016) 4107–4112.  
545 doi:<http://dx.doi.org/10.1016/j.jece.2016.09.019>.
- 546 [11] A. Kumar, A. Rana, G. Sharma, M. Naushad, P. Dhiman, A. Kumari, F.J. Stadler, Recent  
547 advances in nano-Fenton catalytic degradation of emerging pharmaceutical  
548 contaminants, *J. Mol. Liq.* 290 (2019) 111177. doi:10.1016/J.MOLLIQ.2019.111177.
- 549 [12] O. Oral, C. Kantar, Diclofenac removal by pyrite-Fenton process: Performance in batch  
550 and fixed-bed continuous flow systems, *Sci. Total Environ.* (2019).  
551 doi:10.1016/j.scitotenv.2019.02.084.
- 552 [13] G. Ovejero, J.L. Sotelo, F. Martínez, L. Gordo, Novel heterogeneous catalysts in the wet  
553 peroxide oxidation of phenol, *Water Sci. Technol.* 44 (2001) 153–160.  
554 doi:10.2166/wst.2001.0275.
- 555 [14] E. Guélou, J. Barrault, J. Fournier, J.-M. Tatibouët, Active iron species in the catalytic wet  
556 peroxide oxidation of phenol over pillared clays containing iron, *Appl. Catal. B Environ.*  
557 44 (2003) 1–8. doi:10.1016/S0926-3373(03)00003-1.

- 558 [15] M. Munoz, Z.M. de Pedro, N. Menendez, J.A. Casas, J.J. Rodriguez, A ferromagnetic  $\gamma$ -  
559 alumina-supported iron catalyst for CWPO. Application to chlorophenols, *Appl. Catal. B*  
560 *Environ.* 136–137 (2013) 218–224. doi:10.1016/J.APCATB.2013.02.002.
- 561 [16] M. Pariente, R. Molina, F. Martinez Castillejo, J. Melero, J.A. Botas, Heterogeneous  
562 fenton-like processes for the treatment of industrial wastewaters: A review with special  
563 attention to iron-containing silica catalysts, *Water Treat. Process.* (2013) 358–386.
- 564 [17] J.A. Melero, G. Calleja, F. Martínez, R. Molina, Nanocomposite of crystalline Fe<sub>2</sub>O<sub>3</sub> and  
565 CuO particles and mesostructured SBA-15 silica as an active catalyst for wet peroxide  
566 oxidation processes, *Catal. Commun.* 7 (2006) 478–483.  
567 doi:10.1016/J.CATCOM.2006.01.008.
- 568 [18] X. Qian, M. Ren, M. Fang, M. Kan, D. Yue, Z. Bian, H. Li, J. Jia, Y. Zhao, Hydrophilic  
569 mesoporous carbon as iron(III)/(II) electron shuttle for visible light enhanced Fenton-like  
570 degradation of organic pollutants, *Appl. Catal. B Environ.* 231 (2018) 108–114.  
571 doi:10.1016/J.APCATB.2018.03.016.
- 572 [19] A.D. Bokare, W. Choi, Review of iron-free Fenton-like systems for activating H<sub>2</sub>O<sub>2</sub> in  
573 advanced oxidation processes, *J. Hazard. Mater.* 275 (2014) 121–135.  
574 doi:http://dx.doi.org/10.1016/j.jhazmat.2014.04.054.
- 575 [20] M.A. Peña, J.L.G. Fierro, Chemical Structures and Performance of Perovskite Oxides,  
576 *Chem. Rev.* 101 (2001) 1981–2018. doi:10.1021/cr980129f.
- 577 [21] Y. Nie, L. Zhang, Y.-Y. Li, C. Hu, Enhanced Fenton-like degradation of refractory organic  
578 compounds by surface complex formation of LaFeO<sub>3</sub> and H<sub>2</sub>O<sub>2</sub>, *J. Hazard. Mater.* 294  
579 (2015) 195–200. doi:http://dx.doi.org/10.1016/j.jhazmat.2015.03.065.
- 580 [22] K. Rusevova, R. Köferstein, M. Rosell, H.H. Richnow, F.-D. Kopinke, A. Georgi, LaFeO<sub>3</sub> and  
581 BiFeO<sub>3</sub> perovskites as nanocatalysts for contaminant degradation in heterogeneous  
582 Fenton-like reactions, *Chem. Eng. J.* 239 (2014) 322–331.  
583 doi:http://dx.doi.org/10.1016/j.cej.2013.11.025.
- 584 [23] J.. Sotelo, G. Ovejero, F. Martínez, J.. Melero, A. Milieni, Catalytic wet peroxide oxidation  
585 of phenolic solutions over a LaTi<sub>1-x</sub>Cu<sub>x</sub>O<sub>3</sub> perovskite catalyst, *Appl. Catal. B Environ.* 47  
586 (2004) 281–294. doi:10.1016/J.APCATB.2003.09.007.
- 587 [24] K. Soongpravit, D. Aht-Ong, V. Sricharoenchaikul, D. Atong, Synthesis and catalytic activity  
588 of sol-gel derived La-Ce-Ni perovskite mixed oxide on steam reforming of toluene, in:  
589 *Curr. Appl. Phys.*, 2012. doi:10.1016/j.cap.2012.02.025.

- 590 [25] H.J. Wei, Y. Cao, W.J. Ji, C.T. Au, Lattice oxygen of La<sub>1-x</sub>Sr<sub>x</sub>MO<sub>3</sub> (M = Mn, Ni) and LaMnO<sub>3</sub>-  
591 αFβ perovskite oxides for the partial oxidation of methane to synthesis gas, Catal.  
592 Commun. (2008). doi:10.1016/j.catcom.2008.06.019.
- 593 [26] M.R. Carrasco-Díaz, E. Castillejos-López, A. Cerpa-Naranjo, M.L. Rojas-Cervantes, Efficient  
594 removal of paracetamol using LaCu<sub>1-x</sub>MxO<sub>3</sub> (M = Mn, Ti) perovskites as heterogeneous  
595 Fenton-like catalysts, Chem. Eng. J. 304 (2016) 408–418.  
596 doi:http://dx.doi.org/10.1016/j.cej.2016.06.054.
- 597 [27] M.M. Bello, A.A. Abdul Raman, M. Purushothaman, Applications of fluidized bed reactors  
598 in wastewater treatment – A review of the major design and operational parameters, J.  
599 Clean. Prod. 141 (2017) 1492–1514. doi:10.1016/J.JCLEPRO.2016.09.148.
- 600 [28] F. Tisa, A.A. Abdul Raman, W.M.A. Wan Daud, Applicability of fluidized bed reactor in  
601 recalcitrant compound degradation through advanced oxidation processes: A review, J.  
602 Environ. Manage. 146 (2014) 260–275. doi:10.1016/J.JENVMAN.2014.07.032.
- 603 [29] M.I. Pariente, R. Molina, J.A. Melero, J.Á. Botas, F. Martínez, Intensified-Fenton process  
604 for the treatment of phenol aqueous solutions, Water Sci. Technol. 71 (2015).  
605 doi:10.2166/wst.2014.515.
- 606 [30] C. Kantar, O. Oral, N.A. Oz, Ligand enhanced pharmaceutical wastewater treatment with  
607 Fenton process using pyrite as the catalyst: Column experiments, Chemosphere. 237  
608 (2019) 124440. doi:10.1016/J.CHEMOSPHERE.2019.124440.
- 609 [31] F. Martínez, R. Molina, I. Rodríguez, M.I. Pariente, Y. Segura, J.A. Melero, Techno-  
610 economical assessment of coupling Fenton/biological processes for the treatment of a  
611 pharmaceutical wastewater, J. Environ. Chem. Eng. 6 (2018).  
612 doi:10.1016/j.jece.2017.12.008.
- 613 [32] T. Fey, U. Betke, S. Rannabauer, M. Scheffler, Reticulated Replica Ceramic Foams:  
614 Processing, Functionalization, and Characterization, Adv. Eng. Mater. (2017).  
615 doi:10.1002/adem.201700369.
- 616 [33] Y. Yao, T. Ochiai, H. Ishiguro, R. Nakano, Y. Kubota, Antibacterial performance of a novel  
617 photocatalytic-coated cordierite foam for use in air cleaners, Appl. Catal. B Environ. 106  
618 (2011) 592–599. doi:10.1016/J.APCATB.2011.06.020.
- 619 [34] G. Plesch, M. Vargová, U.F. Vogt, M. Gorbár, K. Jesenák, Zr doped anatase supported  
620 reticulated ceramic foams for photocatalytic water purification, Mater. Res. Bull. 47  
621 (2012) 1680–1686. doi:10.1016/J.MATERRESBULL.2012.03.057.

- 622 [35] S. Josset, S. Hajiesmaili, D. Begin, D. Edouard, C. Pham-Huu, M.-C. Lett, N. Keller, V. Keller,  
623 UV-A photocatalytic treatment of Legionella pneumophila bacteria contaminated  
624 airflows through three-dimensional solid foam structured photocatalytic reactors, J.  
625 Hazard. Mater. 175 (2010) 372–381. doi:10.1016/J.JHAZMAT.2009.10.013.
- 626 [36] A. Kocakuşakoğlu, M. Dağlar, M. Konyar, H.C. Yatmaz, K. Öztürk, Photocatalytic activity  
627 of reticulated ZnO porous ceramics in degradation of azo dye molecules, J. Eur. Ceram.  
628 Soc. 35 (2015) 2845–2853. doi:10.1016/J.JEURCERAMSOC.2015.03.042.
- 629 [37] K.I. Ekpeghere, W.J. Sim, H.J. Lee, J.E. Oh, Occurrence and distribution of carbamazepine,  
630 nicotine, estrogenic compounds, and their transformation products in wastewater from  
631 various treatment plants and the aquatic environment, Sci. Total Environ. (2018).  
632 doi:10.1016/j.scitotenv.2018.05.218.
- 633 [38] Y. Zhang, S.U. Geißen, C. Gal, Carbamazepine and diclofenac: Removal in wastewater  
634 treatment plants and occurrence in water bodies, Chemosphere. (2008).  
635 doi:10.1016/j.chemosphere.2008.07.086.
- 636 [39] H. Haugen, J. Will, A. Köhler, U. Hopfner, J. Aigner, E. Wintermantel, Ceramic TiO<sub>2</sub>-foams:  
637 characterisation of a potential scaffold, J. Eur. Ceram. Soc. 24 (2004) 661–668.  
638 doi:10.1016/S0955-2219(03)00255-3.
- 639 [40] F. Martínez, J.A. Melero, J.Á. Botas, M. Isabel Pariente, R. Molina, Treatment of phenolic  
640 effluents by catalytic wet hydrogen peroxide oxidation over  
641 Fe<sub>2</sub>O<sub>3</sub>/SBA-15 extruded catalyst in a fixed-bed reactor, Ind. Eng.  
642 Chem. Res. 46 (2007). doi:10.1021/ie070165h.
- 643 [41] A. Cruz del Álamo, M.I. Pariente, F. Martínez, R. Molina, Trametes versicolor immobilized  
644 on rotating biological contactors as alternative biological treatment for the removal of  
645 emerging concern micropollutants, Water Res. 170 (2020) 115313.  
646 doi:10.1016/J.WATRES.2019.115313.
- 647 [42] Y.N. Lee, R.M. Lago, J.L.G. Fierro, J. González, Hydrogen peroxide decomposition over  
648 Ln<sub>1-x</sub>A<sub>x</sub>MnO<sub>3</sub> (Ln = La or Nd and A = K or Sr) perovskites, Appl. Catal. A Gen. (2001).  
649 doi:10.1016/S0926-860X(01)00536-1.
- 650 [43] A. Babuponnusami, K. Muthukumar, A review on Fenton and improvements to the  
651 Fenton process for wastewater treatment, J. Environ. Chem. Eng. 2 (2014) 557–572.  
652 doi:10.1016/J.JECE.2013.10.011.
- 653 [44] G. Wen, S.J. Wang, J. Ma, T.L. Huang, Z.Q. Liu, L. Zhao, J.L. Xu, Oxidative degradation of



654 organic pollutants in aqueous solution using zero valent copper under aerobic  
655 atmosphere condition, *J. Hazard. Mater.* (2014). doi:10.1016/j.jhazmat.2014.05.002.

656 [45] J.A. Melero, G. Calleja, F. Martínez, R. Molina, Nanocomposite of crystalline Fe<sub>2</sub>O<sub>3</sub> and  
657 CuO particles and mesostructured SBA-15 silica as an active catalyst for wet peroxide  
658 oxidation processes, *Catal. Commun.* 7 (2006). doi:10.1016/j.catcom.2006.01.008.

659 [46] S.P. Sun, X. Zeng, A.T. Lemley, Kinetics and mechanism of carbamazepine degradation by  
660 a modified Fenton-like reaction with ferric-nitrilotriacetate complexes, *J. Hazard. Mater.*  
661 (2013). doi:10.1016/j.jhazmat.2013.02.045.

662 [47] S.P. Sun, X. Zeng, A.T. Lemley, Nano-magnetite catalyzed heterogeneous Fenton-like  
663 degradation of emerging contaminants carbamazepine and ibuprofen in aqueous  
664 suspensions and montmorillonite clay slurries at neutral pH, *J. Mol. Catal. A Chem.*  
665 (2013). doi:10.1016/j.molcata.2013.01.027.

666 [48] Y. Ding, H. Tang, S. Zhang, S. Wang, H. Tang, Efficient degradation of carbamazepine by  
667 easily recyclable microscaled CuFeO<sub>2</sub> mediated heterogeneous activation of  
668 peroxymonosulfate, *J. Hazard. Mater.* (2016). doi:10.1016/j.jhazmat.2016.06.004.

669 [49] R. Bulánek, R. Hrdina, A.F. Hassan, Preparation of polyvinylpyrrolidone modified  
670 nanomagnetite for degradation of nicotine by heterogeneous Fenton process, *J. Environ.*  
671 *Chem. Eng.* (2019). doi:10.1016/j.jece.2019.102988.

672 [50] Y. Shao, H. Chen, Heterogeneous Fenton oxidation of phenol in fixed-bed reactor using  
673 Fe nanoparticles embedded within ordered mesoporous carbons, *Chem. Eng. Res. Des.*  
674 132 (2018) 57–68. doi:10.1016/J.CHERD.2017.12.039.

675 [51] C. di Luca, P. Massa, J.M. Grau, S.G. Marchetti, R. Fenoglio, P. Haure, Highly dispersed Fe  
676 3+ -Al<sub>2</sub>O<sub>3</sub> for the Fenton-like oxidation of phenol in a continuous up-flow fixed bed  
677 reactor. Enhancing catalyst stability through operating conditions, *Appl. Catal. B Environ.*  
678 (2018). doi:10.1016/j.apcatb.2018.05.032.

679 [52] L.H.M.L.M. Santos, M. Gros, S. Rodriguez-Mozaz, C. Delerue-Matos, A. Pena, D. Barceló,  
680 M.C.B.S.M. Montenegro, Contribution of hospital effluents to the load of  
681 pharmaceuticals in urban wastewaters: Identification of ecologically relevant  
682 pharmaceuticals, *Sci. Total Environ.* 461–462 (2013) 302–316.  
683 doi:10.1016/J.SCITOTENV.2013.04.077.

684 [53] N. Collado, S. Rodriguez-Mozaz, M. Gros, A. Rubirola, D. Barceló, J. Comas, I. Rodriguez-  
685 Roda, G. Buttiglieri, Pharmaceuticals occurrence in a WWTP with significant industrial

686 contribution and its input into the river system, *Environ. Pollut.* 185 (2014) 202–212.  
687 doi:<https://doi.org/10.1016/j.envpol.2013.10.040>.

688